Available online at www.sciencedirect.com
ScienceDirect
Earth and Planetary Science Letters 269 (2008) 17–28
EPSL
www.elsevier.com/locate/epsl

Zinc stable isotopes in seafloor hydrothermal vent fluids and chimneys

Seth G. John [a,*], Olivier J. Rouxel [b], Paul R. Craddock [c], Alison M. Engwall [d], Edward A. Boyle [d]

[a] Massachusetts Institute of Technology/Woods Hole Oceanographic Institution Joint Program in Chemical Oceanography, Massachusetts Institute of Technology, MIT E34-272, Cambridge, Massachusetts 02139, USA
[b] Marine Chemistry and Geochemistry Department, Woods Hole Oceanographic Institution, Clark 403, MS#25, Woods Hole, MA 02543, USA
[c] Massachusetts Institute of Technology/Woods Hole Oceanographic Institution Joint Program in Chemical Oceanography, Marine Chemistry and Geochemistry Department, Woods Hole Oceanographic Institution, McLean 201, MS#8, Woods Hole, MA 02543, USA
[d] Department of Earth, Atmospheric, and Planetary Sciences, Massachusetts Institute of Technology, Cambridge, Massachusetts 02139, USA

Received 17 July 2007; received in revised form 6 December 2007; accepted 10 December 2007
Available online 23 December 2007
Editor: M.L. Delaney

Abstract

Many of the heaviest and lightest natural zinc (Zn) isotope ratios have been discovered in hydrothermal ore deposits. However, the processes responsible for fractionating Zn isotopes in hydrothermal systems are poorly understood. In order to better assess the total range of Zn isotopes in hydrothermal systems and to understand the factors which are responsible for this isotopic fractionation, we have measured Zn isotopes in seafloor hydrothermal fluids from numerous vents at 9–10°N and 21°N on the East Pacific Rise (EPR), the TAG hydrothermal field on the Mid-Atlantic Ridge, and in the Guaymas Basin. Fluid δ^{66}Zn values measured at these sites range from +0.00‰ to +1.04‰. Of the many physical and chemical parameters examined, only temperature was found to correlate with fluid δ^{66}Zn values. Lower temperature fluids (<250 °C) had both heavier and more variable δ^{66}Zn values compared to higher temperature fluids from the same hydrothermal fields. We suggest that subsurface cooling of hydrothermal fluids leads to precipitation of isotopically light sphalerite (Zn sulfide), and that this process is a primary cause of Zn isotope variation in hydrothermal fluids. Thermodynamic calculations carried out to determine saturation state of sphalerite in the vent fluids support this hypothesis with isotopically heaviest Zn found in fluids that were calculated to be saturated with respect to sphalerite. We have also measured Zn isotopes in chimney sulfides recovered from a high-temperature (383 °C) and a low-temperature (203 °C) vent at 9–10°N on the EPR and, in both cases, found that the δ^{66}Zn of chimney minerals was lighter or similar to the fluid δ^{66}Zn. The first measurements of Zn isotopes in hydrothermal fluids have revealed large variations in hydrothermal fluid δ^{66}Zn, and suggest that subsurface Zn sulfide precipitation is a primary factor in causing variations in fluid δ^{66}Zn. By understanding how chemical processes that occur beneath the seafloor affect hydrothermal fluid δ^{66}Zn, Zn isotopes may be used as a tracer for studying hydrothermal processes.

Keywords: hydrothermal; trace metals; isotopic fractionation; Zn isotopes; sulfide

1. Introduction

With the advent of multi-collector inductively coupled plasma mass spectrometry (ICPMS), stable isotope variability of transition metals has been seen in many natural samples (Johnson et al., 2004; Anbar and Rouxel, 2007). Zinc (Zn) isotopes have been studied in rocks (Maréchal et al., 2000; Chapman et al., 2006), marine sediments (Pichat et al., 2003), biological materials (Maréchal et al., 2000; Weiss et al., 2005), seawater (Bermin et al., 2006), and ore deposits (Mason et al., 2005; Wilkinson et al., 2005). Several metal and metalloid isotopes have been studied in active hydrothermal systems include iron (Fe) isotopes (Sharma et al., 2001; Rouxel et al., 2004b; Severmann et al., 2004), copper (Cu) isotopes (Zhu et al., 2000; Rouxel et al., 2004a), molybdenum (Mo) isotopes (McManus et al., 2002), selenium (Se) isotopes (Rouxel et al., 2004b), and antimony (Sb) isotopes (Rouxel et al., 2003). By

* Corresponding author. Tel.: +1 617 253 5739; fax: +1 617 253 8630.
E-mail addresses: sjohn@mit.edu (S.G. John), orouxel@whoi.edu (O.J. Rouxel), pcraddock@whoi.edu (P.R. Craddock), aengwall@mit.edu (A.M. Engwall), eaboyle@mit.edu (E.A. Boyle).

0012-821X/$ - see front matter © 2008 Elsevier B.V. All rights reserved.
doi:10.1016/j.epsl.2007.12.011

studying the distribution of Zn isotopes in hydrothermal systems it is hoped that they can be also used as tracers of seafloor hydrothermal processes, helping us to better understand the plumbing and chemistry of hydrothermal vents.

Zn isotope measurements in ancient hydrothermal deposits have uncovered large variations in δ^{66}Zn values of sulfide minerals, including both the heaviest and lightest Zn isotope samples reported to date (δ^{66}Zn=−0.43‰ and δ^{66}Zn=+1.33‰) (Mason et al., 2005; Wilkinson et al., 2005). Thorough studies of Zn isotopes carried out in the Alexandrinka volcanic-hosted massive sulfide ore deposit in Urals, Russia (Mason et al., 2005) and the Irish Midlands ore field (Wilkinson et al., 2005) have related Zn isotopes to hydrothermal processes. The Alexandrinka ore deposit was formed as a seafloor hydrothermal system similar to modern systems studied here. Samples from the Alexandrinka deposit were analyzed from the hydrothermal-metasomatic stockwork believed to be the feeder zone to the hydrothermal deposit, a seafloor chimney, and some clastic sediments. δ^{66}Zn values from the deposit ranged from −0.43‰ to +0.23‰. A systematic increase in δ^{66}Zn values from the chimney core to the chimney rim was attributed to either a temperature dependence in the fractionation factor for precipitation or Rayleigh distillation as fluids diffuse through the chimney wall. Zn isotopes in the Irish Midlands ore field show a general trend of lighter Zn isotopes precipitated in the deep feeder veins and heavier Zn isotopes near the top of the hydrothermal system. Based on these data, Wilkinson et al. (2005) were the first to suggest that the precipitation of isotopically light Zn into Zn sulfides could influence the δ^{66}Zn of hydrothermal samples. Other studies have investigated Zn isotopes in sulfides from various ore deposits (Maréchal et al., 1999; Albarède, 2004) and in sulfides recovered from Archean shales (Archer and Vance, 2002).

While studies of extinct hydrothermal systems have suggested several processes that may fractionate Zn isotopes, it can be difficult to distinguish which of these effects are most important. It is hoped that the study of Zn isotopes at active vents will elucidate the processes that most influence hydrothermal δ^{66}Zn by allowing δ^{66}Zn to be directly related to the physical (i.e. temperature) and chemical properties that document subsurface hydrothermal processes. We have chosen samples from a wide range of hydrothermal vent sites in order to establish the range in hydrothermal fluid δ^{66}Zn values and to constrain the hydrothermal conditions under which Zn isotopes are fractionated. At two sites, we have investigated the Zn-isotope composition of hydrothermal fluids and Zn sulfide minerals from the same vent, providing further constraints on how sulfide precipitation may fractionate Zn isotopes in hydrothermal systems.

2. Geologic settings and sample description

Samples analyzed in this study were selected from several distinct geographic regions along basalt-hosted mid-ocean ridges, including from the fast-spreading, unsedimented East-Pacific Rise (9–10°N and 21°N EPR), from the sedimented Gulf of California (Guaymas basin) and from the slow spreading Mid-Atlantic ridge (TAG Active Mound). The 9–10°N EPR site is located in a well-studied segment of the EPR between the Clipperton and Siqueiros Fracture Zones (Haymon et al., 1991; Haymon et al., 1993; Fornari et al., 1998; Shank et al., 1998; Von Damm, 2000; Von Damm and Lilley, 2004; Von Damm, 2004). The vent fluid chemistry in the area has been well documented and previous studies have reported temporal evolution of the vent systems since 1991 in relation to magmatic events (Von Damm et al., 1997; Von Damm, 2004). Hence, hydrothermal vents at EPR 9–10°N provide a unique opportunity to study Zn-isotope systematics in one of the youngest hydrothermal systems. Bio9'' vent is located at 9°50' N within an area where dramatic changes in the hydrothermal systems have taken place. In 1991, Bio9 was the only high-temperature vent sampled in the Bio9 area. By 1994, Bio9' vent was another distinct black smoker. By 1999, the number of smokers around Bio9 had further increased, replacing some of the areas that had previously been characterized by diffuse flow. Bio9" is the third distinct smoker in the Bio9 area and was initially sampled in 2002. K-vent at 9°30' N is the most southerly active vent, before encountering a zone of extinct vents (Von Damm, 2000). Fluids from K-vent discharge at a distinctly lower temperature than other vents in this area. Present temperatures are even lower than the temperature reported in 1991 (263 °C) (Von Damm, 2000). At K-vent, the entire active chimney was removed and the fluids were subsequently sampled from the remaining base of the chimney. The 21°N EPR site was among the first ridge-crest hydrothermal systems to be studied (Von Damm et al., 1985a). Three of the vent sites (Ocean Bottom Seismometer (OBS), South West (SW), and Hanging Gardens (HG)) were typical high-temperature black smokers and their chemical composition remained quite stable over the three years between 1979 and 1981 (Campbell et al., 1988). The fourth (National Geographic Society (NGS)) was a black smoker when originally sampled in 1979 but had become sealed off when revisited in 1981 and it emitted low-temperature white smoker fluids when broken open. The Guaymas basin in the Gulf of California is also located along the EPR, but in contrast to 9–10°N and 21°N EPR sites, it is covered by a thick layer of sediment through which hydrothermal fluids pass before venting on the seafloor. The TAG hydrothermal field lies on the more slowly spreading Mid-Atlantic Ridge. This site is distinguished by the large extent of subsurface remobilization of previously deposited Zn sulfide, which is evidenced by Zn-rich compositions of white smoker fluids and chimney sulfides compared to high-temperature black smokers (Tivey et al., 1995).

In addition to hydrothermal fluid samples, two hydrothermal deposits were studied at EPR 9–10°N and include: (1) Cu-rich chimneys (black smokers) from Bio9'', and (2) Zn-and Fe-rich chimneys and diffusers from K-vent. Reflected light microscopy was used for mineral identification and textural interpretations, description of each hydrothermal deposit types are presented in more detailed in a companion paper (Rouxel et al., in press).

Deposits characterized by abundant Cu-rich sulfide (i.e. chalcopyrite) and are typical of black smokers such as Bio9'' that formed at temperatures higher than 300 °C. The hydrothermal chimney recovered at Bio9'' has a wide trunk (~40 cm wide) that bifurcates into two orifices, one that was venting vigorously, and a second inactive one. Sample ALV-4057-M1 represents the

uppermost 40–50 cm of the black smoker, venting fluid at a temperature of 383 °C (fluid samples ALV-4057-W1&W2). The entire sample M1 has been divided into various pieces (#A1 to #A6 and #B1) that represent sections from bottom to top. M1 is characterized by a well-zoned mineralogy across the chimney wall that varies in thickness from 1 to 4 cm. All samples are characterized by a thick inner layer of euhedral to massive chalcopyrite. Anhydrite is ubiquitously associated with chalcopyrite within the chimney wall but may also occur as cm-wide patches inside the open conduit. The presence of anhydrite reflects active incorporation of seawater and mixing with the high-temperature hydrothermal fluid within the chimney interior (e.g. Tivey, 1995b). The external cm-wide wall is composed mainly of pyrite, marcasite and variable abundance of sphalerite.

The deposit at K-vent is composed of a sulfide mound with numerous little spires that emanate clear fluid. The base is approximately 3 m wide and is heavily colonized by *Alvinella*, sea anemones and vent crabs. Sample ALV-4053-M1 is from the upper part of a spiry chimney. It is 73 cm long and was thickly colonized by *Alvinella*. The removal of the chimney during sampling by Alvin caused vigorous venting of fluid from a small, marcasite-lined orifice with a temperature at about 203 °C. The upper part of the chimney consists of a beehive colonized by *Alvinella* and is composed of sphalerite, pyrite and marcasite and displays multiple tortuous conduits lined with fine-grained sphalerite. Sample ALV-4053-M1 has been divided into 5 sections (#A1 to #A5) from the bottom to the top. Samples #A1 and #A2 correspond to the base of the chimney where the hydrothermal fluid was sampled (fluid samples ALV-4053-W1&W2). The thin (5 mm) chimney wall is composed of euhedral, bladed marcasite with minor sphalerite, galena and chalcopyrite along joints. The exterior of the chimney wall is composed of fine-grained pyrite with variable enrichment of marcasite, sphalerite and minor galena. Samples A3 to A5 were recovered from the central part of the beehive structure and are composed of euhedral sphalerite along the conduit walls with minor galena and variable enrichment of pyrite and marcasite. Similar mineral assemblages, characterized by significant galena enrichment, which is unusual for unsedimented MOR hydrothermal systems, have been reported previously at K-vent chimney (Peng and Zhou, 2005).

3. Methods

3.1. Sample collection

Samples from the area at 9–10°N EPR were collected in 2004 by the ALVIN submersible (dives 4053 and 4057) during cruise AT11-20 (Rouxel et al., in press). Paired fluid samples and sulfide chimney samples were recovered from both a high-temperature (Bio9'') and lower temperature (K-vent) smoker. Hydrothermal fluid samples from other areas were taken from the collection of John Edmond stored at the Massachusetts Institute of Technology (MIT). Samples from the Pacific were collected from ALVIN dives during 1981–2 cruise to fields at 21°N EPR and Guaymas basin. Geochemical data (pH, alkalinity, and chemical composition) have been reported previously (Von Damm, 1983). Fluids from the TAG Active Mound, Mid-Atlantic Ridge were sampled in 1990. Vents sampled on this cruise included both high-temperature "black smokers" and lower temperature "white smokers". End-member fluids composition (Edmond et al., 1995) and data on dissolved trace-element fluxes have been reported (German et al., 1991). Chemical and physical data for individual samples were provided by Andy Campbell (personal communication, 2007).

All fluid samples in this study were collected using a Ti-syringe with a snorkel that could reach directly into the vent chimney for sampling (Von Damm et al., 1985a). Due to the high concentrations of metals in the hydrothermal solutions, precipitation often occurs within the titanium samplers as they cool to ambient temperature. For samples collected from 9–10°N on the EPR, those insoluble or precipitated particles remaining in the Ti-samplers were recovered when the samplers were disassembled by rinsing with Milli-Q water onto 0.45 μm filters and saving this fraction for chemical analysis. This fraction is hereafter called "dregs". Fluids from the 9–10°N site were acidified with concentrated HCl to pH ~1. For samples from the MIT hydrothermal vent fluid collection, it was believed at the time of sampling that precipitation of sulfides inside of the Ti-syringe was not significant, and that when sulfides did form in the sampler they could be redissolved in the storage bottle by the addition of 6 N HCl to a pH of about 1.6. In fact, these early sampling methods may have left some particles (dregs) behind in the syringes. All of the MIT samples were observed at the time of collection to be clear following acidification.

For all fluid samples, the highest recorded temperature from the vent field was used instead of the temperature recorded for any individual sample. Individual temperature measurements were quite difficult with the ALVIN temperature probe (Campbell et al., 1988).

3.2. Sample processing

All samples were processed under class-100 clean air flow. All acids were quadrupally distilled in Vycor glass and water was either Milli-Q or distilled in borosilicate glass.

3.2.1. Hydrothermal fluids

Vent fluids from the MIT collection were mixed with 6N HCl to a concentration of 2 M Cl^- for purification by anion exchange chromatography. Because vent fluids from the 9–10°N site contained significant particulates (black crystalline particles presumed to be metal sulfides that formed during sample storage, i.e. after separation from the "dregs"), 12 mL of the homogenized fluid-particle mixture was reacted overnight in a closed PFA capsule with 3 mL 14N HNO_3 and 3 mL 6N HCl in order to oxidize and dissolve precipitates. The solution was diluted to 20 mL with a Cl^- concentration of 2 M for column purification.

Many of the MIT samples had a small amount (less than a gram) of a clear crystalline precipitate in the bottom. These samples had been filtered upon collection, so the precipitate must have formed during sample storage. The composition of the precipitate is unknown, but it could be amorphous silica or elemental sulfur. This precipitate was separated from 10 mL of homogenized fluid by centrifugation and redissolved in 2% HNO_3 for elemental

analysis. Elemental measurements were performed on a Plasma-Quad 2+ quadrupole ICP-MS (VG Elemental, now Thermo Electron) using an In spike to correct for signal suppression. In all fluids the amount of Zn in the precipitate was less than 0.1% of the dissolved concentration.

3.2.2. Chimney sulfides

Hydrothermal sulfide samples were crushed between two plexiglass discs inside a Teflon bag using a hydraulic press. Sulfide grains were collected between 500 μm and 1.0 mm sieves and monomineralic sulfide phases were isolated by hand picking under a microscope. For each sample, between 15 and 50 mg of sulfide was picked in order to obtain a representative sample. Care was taken to select pure sulfide grains without other mineral inclusions but in most cases inclusions were unavoidable, especially for sphalerite (ZnS) which includes other phases such as pyrite and chalcopyrite (Table 1). Samples were weighted in 15 mL Teflon beakers and dissolved using 5 mL of concentrated HNO_3. After evaporation on a hot plate at 60 °C, complete dissolution was achieved by a second evaporation step using 5 mL of aqua regia. Dry residue was dissolved in 5 mL of 6N HCl with trace H_2O_2 by heating at 40 °C in a closed vessel and diluted to a concentration of 2 M Cl^- before purification.

Table 1
Mineralogical and Zn isotopic analyses were carried out on each of the chimney sulfide samples

Sample ID	Mineralogy	Zn (wt.%)	Cd (ppm)	Cu (wt.%)	Fe (wt.%)	δ^{66} Zn	±2σ s.d.
Bio 9''(Cu-rich chimneys)							
ALV-4057-M1 #A1	cpy	0.09	2	27.11	29.0	0.17	0.04
ALV-4057-M1 #A1	sph-py	22.67	611	0.59	26.3	0.07	0.04
ALV-4057-M1 #B1	cpy	0.05	2	30.81	28.9	0.16	0.02
ALV-4057-M1 #A3	cpy	0.15	6	29.09	29.3	0.09	0.03
ALV-4057-M1 #A3	sph-py	23.98	480	1.88	26.3	0.27	0.01
ALV-4057-M1 #A4	cpy	0.13	5	29.34	28.1	−0.09	0.02
ALV-4057-M1 #A4	sph-py	26.51	714	2.32	21.1	0.02	0.01
ALV-4057-M1 #A5	cpy	0.04	1	27.32	26.5	0.14	0.02
ALV-4057-M1 #A5	sph-py	22.90	634	0.64	25.5	0.32	0.01
ALV-4057-M1 #A6	cpy	0.02	1	31.68	29.0	0.27	0.03
K-vent (Active Fe-Zn-rich chimneys and diffusers)							
ALV-4053-M1 #A1	sph-py-ga	24.82	1174	1.16	10.6	0.60	0.04
ALV-4053-M1 #A2b	sph-py-ga	20.88	609	0.69	10.2	1.03	0.01
ALV-4053-M1 #A2t	sph-py-ga	8.90	198	0.16	9.7	1.13	0.02
ALV-4053-M1 #A4	py-sph	11.47	162	0.15	23.3	1.17	0.01
ALV-4053-M1 #A5	py-sph	13.22	259	0.17	27.5	0.57	0.03

The percentage elemental composition is presented along with a description of the dominant minerals present (cpy=chalcopyrite, sph=sphalerite, py=pyrite, ga=galena). δ^{66}Zn values are given with the internal error (2σ s.d.) for triplicate analysis of a single sample.

3.2.3. Purification by anion exchange chromatography

Samples were purified by anion exchange chromatography using a procedure modified from that of Maréchal et al. (1999). Samples were loaded in 2 N HCl in order to minimize the amount of acid used and decrease the chance of premature elution, as the affinity of Zn for the resin is highest at 2 N HCl (Kraus and Moore, 1953). Samples were rinsed with 15 mL 2 N HCl to remove sea salts and other contaminants. Zn was eluted in 12 mL 0.06 N HCl (rather than 0.5 N HNO_3), which may help avoid elution of other elements (Chapman et al., 2006). Samples were evaporated to dryness in 15 mL PFA capsules, and reacted at high heat overnight with 200 μL concentrated HNO_3 and 100 μL concentrated HF to remove residual silicates from the sample and residual organics that may have leached from the column. Zn recovery was determined by graphite furnace atomic absorption spectrometry using a Hitachi Z-8100 spectrophotometer.

3.3. Isotopic analysis

3.3.1. Isotope ratio measurements

Samples were redissolved in 2% HNO_3 at a Zn concentration of 50, 100, or 200 ppb for isotopic analysis. All samples were analyzed with 100 ppb Cu (Ultra Scientific, Lot #D00204) for instrumental mass fractionation correction. Isotope ratio measurements were made on an IsoProbe multi-collector ICP-MS (Thermo Fisher, formerly Micromass) using an APEX Q inlet system (ESI) with a 75 μL min^{-1} MicroMist nebulizer (Glass Expansion) in soft extraction mode. The optional desolvating membrane was not used as we have sometimes observed large variations in mass bias when using it, an effect that has also been observed with the Aridus (CETAC) (Archer and Vance, 2004). Signal intensity was measured on masses 60, 63, 64, 65, 66, 67, and 68 using Faraday collectors in fifteen blocks of ten seconds. $^{64}Ni^+$ was subtracted from the $^{64}Zn^+$ signal by monitoring the signal from $^{60}Ni^+$. Because we used Al sampling cones, the corrections for Ni were insignificant (<5 μV with ^{64}Zn signals from 0.5–2 V). All peaks were corrected for acid blanks using an on-peak zero immediately prior to measurement. All Zn isotope data are reported in terms of deviation from the "Lyon JMC" Zn standard.

Data were corrected for instrumental mass bias using the Cu internal spike. The relationship between Cu and Zn instrumental fractionation has been shown to differ from predictions of the exponential mass bias law (Maréchal et al., 1999; Albarède and Beard, 2004). A linear relationship between the natural log of $^{65}Cu/^{63}Cu$ and $^{66}Zn/^{64}Zn$ in standards was used instead to determine the mass bias relationship (Fig. 1, Supplementary data). Because variations in instrumental mass fractionation are greatly reduced with the removal of the desolvator from the APEX, modified standards containing H_2SO_4, Sr, or organics leached from polyethylene bottles after many months of storage

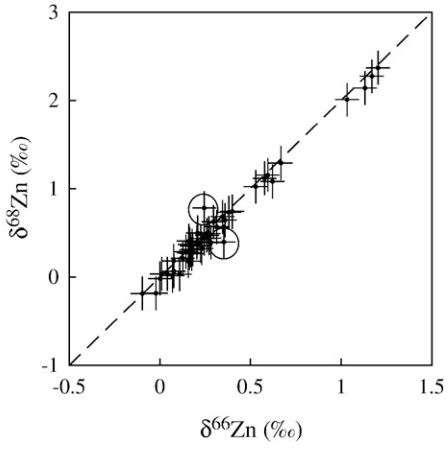

Fig. 1. Comparison of sample δ^{68}Zn and δ^{66}Zn demonstrates the absence of isobaric interferences. The dashed line represents the expected 2:1 relationship between δ^{68}Zn and δ^{66}Zn. The two outliers (circled) were measured twice and had matching δ^{66}Zn values, suggesting that the error lay in δ^{68}Zn. There appears to be a small unexplained bias towards heavy δ^{66}Zn compared to the values predicted by δ^{68}Zn. Error bars were calculated from the pooled standard deviation of several standards processed as samples, and several samples run during different analytical sessions (±0.069‰ δ^{66}Zn;±0.192‰ δ^{68}Zn; 2σ).

were sometimes used to artificially increase mass bias (Archer and Vance, 2004). All samples were measured in triplicate and were corrected for mass bias using Cu. Sample standard bracketing with Cu-corrected samples and standards was used to obtain the final values.

Mass bias was also corrected on several samples using a Zn double spike. A spike mixed predominantly from ^{64}Zn and ^{67}Zn was used added to samples such that the sample-spike mixture had a ^{64}Zn:^{66}Zn:^{67}Zn:^{68}Zn ratio of 4.2: 1.3: 1.6: 1. This ratio was optimized according to standard procedures to minimize our analytical error (Galer, 1999). Isotope ratios were calculated using a Newton Raphson iteration (Albarède and Beard, 2004).

3.3.2. Error analysis

Error was estimated by calculating the pooled standard deviation of seven samples that were purified and analyzed in duplicate, combined with the analytical error for five process standards. The calculated external error was 0.069‰ (2σ s.d.). The average internal error for triplicate analysis of samples measured in this study was 0.034‰ (2σ s.d.). There was no apparent difference in the magnitude of internal error of triplicate analysis between hundreds of samples run at 50, 100, and 200 ppb.

Data were checked for polyatomic or doubly charged interferences by comparing δ^{66}Zn values to δ^{68}Zn values (Fig. 1). With two exceptions, the data show the expected trend in mass bias within error. These two samples were run twice and the discrepancy between the two runs lies in the δ^{68}Zn values, indicating that the δ^{66}Zn values are accurate. The values obtained by correcting for instrumental mass bias using a double spike matched those corrected for mass bias using Cu, indicating that both mass bias corrections are robust (Fig. 2). For fluids from Bio" and K-vent at 9–10°N EPR, duplicate samples were collected with Ti-syringes; the isotopic composition of these fluids is identical within our analytical precision (Table 2).

3.4. Vent fluid modeling

Thermodynamic calculations were performed for each fluid composition to determine the equilibrium speciation of dissolved species, the saturation state (log Q/K) of sphalerite at *in situ* conditions (i.e., of the conditions during vent fluid discharge from chimney edifices), and the temperature at which sphalerite would be saturated (log $Q/K=0$) if the fluid cooled via conduction. Calculations were carried out using the computer program EQ3/6 (Wolery, 1992; Wolery and Daveler, 1992), incorporating the SUPCRT92 database (Johnson et al., 1992). Modifications to the SUPCRT92 database included addition of Na_2SO_4 and $MgSO_4$ species (McCollom and Shock, 1997), $HCl_{(aq)}$ (Sverjensky et al., 1991), and $FeCl_{2(aq)}$ and $CuCl_{(aq)}$ at temperatures above 300 °C (Ding and Seyfried, 1992a,b). Data for fluids from 21°N EPR and Guaymas basin are taken from Von Damm (1983), Von Damm et al. (1985a,b) and Welhan and Craig (1983). Data for black smoker fluids from the TAG active mound are from Edmond et al. (1995). For white smoker fluids from the TAG active mound, fluid speciation calculations have been performed previously (Tivey et al., 1995) and are replicated here. For K-vent and Bio9" fluids from 9–10°N EPR, data are from Rouxel et al. (in press), excluding dissolved gaseous species ($CO_{2(aq)}$, $H_2S_{(aq)}$, $H_{2(aq)}$) for which compositions are estimated from the chlorinity, assuming the same regressions between chlorinity and $CO_{2(aq)}$, $H_2S_{(aq)}$ and $H_{2(aq)}$ observed for all other 9–10°N EPR fluids detailed in Von Damm (2004) and Von Damm and Lilley (2004). Fluid compositions used in calculations are shown in Table 3. Note that for TAG white smoker and K-vent fluids, Mg concentrations of fluids exiting the vents are not assumed to be zero, but are instead assumed to be 7.4 mmol/kg due to subsurface mixing with seawater (Tivey et al., 1995). At K-vent, Mg concentrations are assumed to be ~3 mmol/kg due to local entrainment of seawater into the diffusive chimney structure (Rouxel et al., in press).

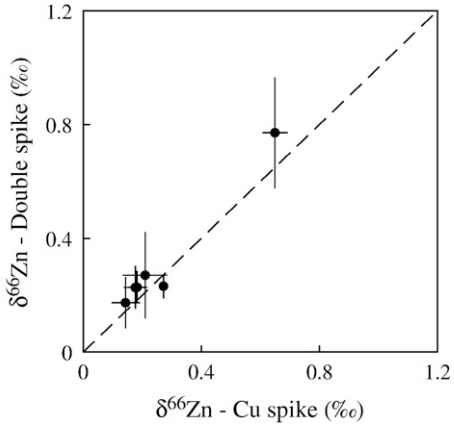

Fig. 2. Comparison of δ^{66}Zn values measured using either a Zn double spike method or an internal Cu spike to correct for instrumental mass bias. Within the analytical error, values provided by both methods are in agreement. The dashed line represent the 1:1 relationship between values for these two different methods. Error bars represent the internal error for triplicate analysis of each individual sample (1σ).

Table 2
Hydrothermal fluid samples were analyzed for elemental concentrations and Zn isotope composition

Site	Vent name	Sample ID	Temp (°C)	Mg (mmol/kg)	Zn (μmol/kg)	δ^{66}Zn	±2σs.d.
Sampler fluids							
EPR 21°N	SW	1149-1	355	2.13	95	0.13	0.09
EPR 21°N	SW	1149-1	355	2.13	95	0.16	0.01
EPR 21°N	SW	1153-9	355	3.60	91	0.27	0.02
EPR 21°N	NGS	1151-6	273	2.90	39	0.62	0.04
EPR 21°N	NGS	1151-6	273	2.90	39	0.68	0.05
EPR 21°N	NGS	1151-14	273	17.21	38	0.25	0.02
EPR 21°N	NGS	1155-1	273	2.10	39	0.55	0.03
EPR 21°N	OBS	1152-16	350	6.75	81	0.18	0.04
EPR 21°N	OBS	1158-16	350	1.14	112	0.21	0.08
EPR 21°N	HG	1160-7	351	2.69	102	0.18	0.04
EPR 21°N	HG	1160-7	351	2.69	102	0.19	0.02
Guaymas	3	1175-9	285	42.26	5	0.33	0.04
TAG	Black smoker	2179-3C	360	28.44		0.20	0.04
TAG	Black smoker	2194-4C	360	27.43		0.00	0.01
TAG	Black smoker	2194-4C	360	27.43		0.05	0.02
TAG	Black smoker	2194-6C	360			0.25	0.07
TAG	White smoker	2187-1C	290	23.24		0.35	0.02
TAG	White smoker	2187-1C	290	23.24		0.41	0.08
TAG	White smoker	2187-4C	290	25.14	116	0.13	0.04
TAG	White smoker	2187-6C	290	27.23	84	0.30	0.02
TAG	White smoker	2187-6C	290	27.23	84	0.31	0.11
EPR 9°N	K-vent	4053 W1	203	8.2	1.5	1.33	0.03
EPR 9°N	K-vent	4053 W2	203	27.3	1.9	1.24	0.03
EPR 9°N	Bio 9''	4057 W1	383	5.3	71.5	0.21	0.03
EPR 9°N	Bio 9''	4057 W1	383	5.3	71.5	0.16	0.00
EPR 9°N	Bio 9''	4057 W2	383	8.5	53.6	0.21	0.01
EPR 9°N	Bio 9''	4057 W2	383	8.5	53.6	0.22	0.05
Sampler dregs							
EPR 9°N	K-vent	dregs (W1)	–		0.6	0.31	0.08
EPR 9°N	K-vent	dregs (W2)	–		1.9	0.34	0.05
EPR 9°N	Bio 9''	dregs (W1)	–		3.7	0.20	0.01
EPR 9°N	Bio 9''	dregs (W2)	–		19.8	0.27	0.05
Original fluids (sampler fluids + dregs)							
EPR 9°N	K-vent	W1 + dregs	–		2.1	1.04	–
EPR 9°N	K-vent	W2 + dregs	–		2.6	0.98	–
EPR 9°N	Bio 9''	W1 + dregs	–		75.1	0.18	–
EPR 9°N	Bio 9''	W2 + dregs	–		73.4	0.23	–

Sample ID is the information written on the sample bottle. Temperatures are the reported end-member vent temperatures (EPR 21°N and Guaymas sample data from Von Damm (1983), TAG sample data from Edmond et al. (1995)). Zn and Mg concentrations are for the unreconstructed fluids (EPR 21°N and Guaymas sample data from Von Damm (1983), TAG sample data from Andy Campbell (pers. comm.)). Where two sets of isotopic data are reported for a single sample, each sample was purified and analyzed separately. The Zn concentration for the dregs is normalized to the volume of the sampler. The isotopic composition of the original fluids is calculated as the sum of the isotopes in the fluids and the fluid dregs. For K-vent sample W2, the concentration and δ^{66}Zn of the original sample is based on the assumption that 71% of the original Zn was dissolved (Section 4.1). δ^{66}Zn and the associated error are from triplicate analysis of a single sample.

For all but the Guaymas Basin fluid, distributions of chemical species were carried out at 25 °C with fixed pH (pH measured shipboard at 25 °C) in order to obtain proton balance conditions. This proton balance was then used to determine *in situ* pH from the re-distribution of chemical species at near *in situ* pressure (250 bars) and temperature conditions (Table 3). For the Guaymas Basin fluid, where CO_2 concentrations are large and pH at 25 °C is relatively high, *in situ* pH was constrained by assuming that the fluid is buffered by calcite (Seewald et al., 1994). The temperature at which sphalerite would be saturated in each fluid ($\log Q/K=0$), if the fluid was conductively cooled, was then calculated by carrying out species distributions at *in situ* and a series of lower temperatures. Note that thermodynamic data exist for the pure ZnS-endmember sphalerite only (i.e., no Zn–Fe solid solution) and are not available for wurtzite.

4. Results and discussion

4.1. Calculating original fluid δ^{66}Zn and Δ^{66}Zn values

For samples collected at 9–10°N EPR, Zn concentrations and δ^{66}Zn were measured separately for dissolved Zn and particulate Zn (dregs) recovered from the samplers. These data were used to reconstruct the isotope composition of the original fluids and to

Table 3
End-member hydrothermal fluid elemental concentrations used for thermodynamic modeling calculations

	9°N EPR [a]			21°N EPR [b]			Guaymas basin [c]	TAG active mound [d]	
	Bio 9"	K-vent	NGS	OBS	SW	HG		1990 BS	990 WS
Temperature (°C)	383	203	273	350	350	350	315	360	290
pH (25 °C)	3.2	4.1	3.8	3.4	3.6	3.3	5.9	3.35	2.84
pH (*in situ*)	4.1	4.5	4.03	4.37	4.56	4.28	5.2	4.38	3.53
Mg (mM)	0.0	3.0	0.0	0.0	0.0	0.0	0.0	0.0	7.4
Cl (mM)	337	666	579	489	496	496	606	636	623
Na (mM)	291	553	508	432	436	443	490	544	540
K (mM)	11.0	27.0	25.8	23.2	23.2	23.9	37.1	17.1	16.1
Ca (mM)	12.0	23.8	20.8	15.6	16.6	11.7	29.5	30.8	25.0
Ba (μM)	–	–	20	8	10	13	24	–	–
SiO_2 (mM)	11.8	10.8	19.5	17.6	17.3	15.6	12.8	20.7	17.8
SO_4 (mM)	0.0	1.6	0.0	0.0	0.0	0.0	0.0	0.0	3.9
Mn (μM)	540	211	1002	960	699	878	139	670	576
Fe (μM)	3584	188	871	1664	750	2439	37	5590	3535
Zn (μM)	85	5	40	106	89	104	2.2	46	344
Cu (μM)	66	1.0	0.02	35	9.7	44	1.1	140	56
Pb (nM)	273	160	183	308	194	359	10	0.3	0.2
CO_2 (mM)	100	25	6.0	6.0	6.0	6.0	40	6.0	5.46
H_2S (mM)	8.2	5.9	6.57	7.3	7.45	8.37	5.1	3.68	0.77
H_2 (mM)	0.37	0.37	0.37	0.37	0.37	0.37	3.0	0.05	1.275
NH_3 (mM)	–	–	–	–	–	–	15.2	–	–
Log Q/K_{sph} (*in situ*)	−2.58	+0.74	−1.20	−2.06	−1.8	−2.24	−1.35	−2.92	−2.86
T of saturation (sph)	194	261	215	209	221	202	265	182	

– = not measured.
[a] 9°N EPR compositions from O. Rouxel et al. (in press), except for SiO_2 (aq) and dissolved gas compositions, which are calculated from chlorinity vs. CO_2, H_2 H_2S and SiO_2 relations in existing 9°N EPR fluids (see Von Damm, 2004 and Von Damm and Lilley, 2004).
[b] 21°N EPR data from Von Damm (1983), Von Damm et al. (1985a) and Welhan and Craig (1983).
[c] Guaymas basin data ("Area 7") from Von Damm (1983), excluding gas data provided by J. Seewald (unpubl.)
[d] TAG black smoker fluid data from Edmond et al. (1995). TAG white smoker fluid data from model results of Tivey et al. (1995), with white smoker fluid extrapolated to Mg=7.4 mM (see text).

calculate the isotope effect for Zn sulfide precipitation in the samplers. $\delta^{66}Zn$ of the original fluid is calculated as the sum of the Zn isotopes in the recovered fluid and particulate fractions as:

$$\delta^{66}Zn_{original} = f \cdot \delta^{66}Zn_{fluid} + (1-f) \cdot \delta^{66}Zn_{dregs}$$

where f is the mass fraction of total Zn in the recovered hydrothermal fluids, and $(1-f)$ was the fraction of Zn recovered in the dregs. $\Delta^{66}Zn$ (sometimes referred to as ε), the instantaneous isotope fractionation factor between fluid and sulfide, was calculated using the Rayleigh isotope distillation equation:

$$\Delta^{66}Zn_{dregs-fluid} = \frac{\delta^{66}Zn_{fluid} - \delta^{66}Zn_{original}}{\ln(f)}.$$

For samples from the Bio9'' site, the $\delta^{66}Zn$ of the fluids and dregs was equal within analytical error, so there was little difference between $\delta^{66}Zn_{fluid}$ and $\delta^{66}Zn_{original,}$ and $\Delta^{66}Zn$ was zero. For samples from K-vent, the Zn concentration measured in the dregs for samples W1 and W2 was very different, though the isotopic composition of fluids and dregs from each sampler was similar (Table 2). Because considerably more seawater was entrained in sample W2, possibly along with more chimney sulfide particles, we assume that not all of the Zn in the dregs from this sample were precipitated from the original hydrothermal fluids. We have therefore applied the value of f from sample W1 (f=0.71) to both samples in order to calculate the $\delta^{66}Zn$ of the original fluids and the isotope fractionation factor for sulfide precipitation in the samplers. $\Delta^{66}Zn$ in these samples was calculated to be −0.87‰ and −0.76‰ for samples W1 and W2, respectively.

4.2. Zinc isotope composition of hydrothermal fluids

Vent fluid samples collected from many different types of hydrothermal systems on EPR and MAR have been analyzed for Zn isotopes (Table 2). Most fluids had $\delta^{66}Zn$ values between +0.1‰ and +0.3‰, though the total range in $\delta^{66}Zn$ for this study was from 0.00‰ to +1.04‰. Many fluid elemental concentrations and physical parameters were compared to $\delta^{66}Zn$ values, but the only significant correlation we discovered was a negative relationship between fluid temperature and $\delta^{66}Zn$ ($p<0.0001$) (Fig. 3). No significant relationship was discovered between $\delta^{66}Zn$ and concentrations of Zn, 1/Zn, Cu, Fe, H_2S, pH, or Fe/Mn (manganese) ratio, although the isotopically heaviest fluids did have among the lowest Cu concentrations (≤1 μM) and Fe/Mn ratios (≤1.3) (Table 1, Supplementary data).

Several explanations can be invoked to explain the variations in fluid $\delta^{66}Zn$, including differences in source-rock $\delta^{66}Zn$, fractionation during phase separation, kinetic or equilibrium fractionation during subsurface precipitation of Zn sulfides, and subsurface redissolution of Zn sulfides. Because the total range of fluid $\delta^{66}Zn$ (0.00‰ to +1.04‰) is an order of magnitude greater than the range of $\delta^{66}Zn$ reported for basalt (+0.20‰ to +0.30‰) (Maréchal et al., 2000; Ben Othman et al., 2003; Archer and Vance, 2004; Chapman et al., 2006), source rocks are not likely

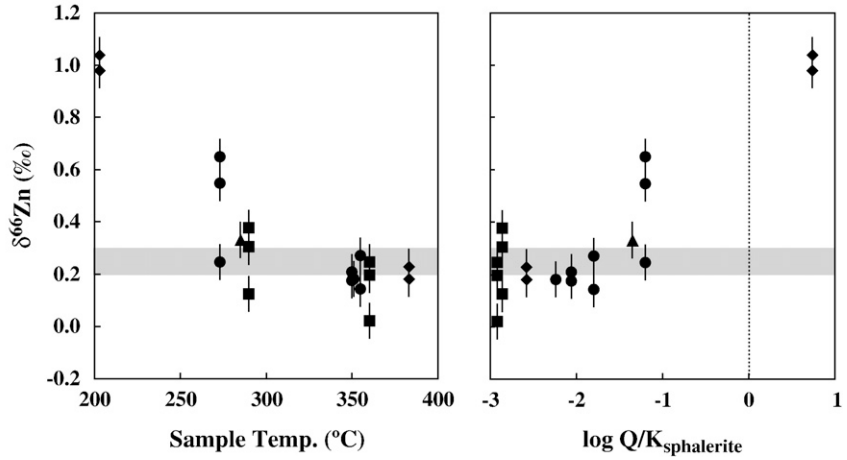

Fig. 3. δ^{66}Zn for vent fluids as a function of fluid temperature and modeled sphalerite saturation. Fluids are from 9–10°N on the EPR (♦), 21°N on the EPR (●), the TAG hydrothermal field (■), and the Guaymas basin (▲). Temperatures are the reported end-members for each vent site (Table 3). Modeled sphalerite solubility is reported as the log of Q (reaction quotient) over K (equilibrium constant), where sphalerite is saturated in the fluids when $Q > K$ (to the right of the dotted line). The grey shaded areas represent the typical δ^{66}Zn range for basalt source rocks (Section 4.2). When samples were purified and analyzed in duplicate, the average isotope ratio is plotted.

the source of isotopic variability. For fluids studied here, phase separation does not appear to be an important factor in fractionating Zn isotopes because we do not observe any relationship between chlorinity and δ^{66}Zn over a range of Cl^- from 337 mM at K-vent to 673 mM at Bio9".

We hypothesize that subsurface precipitation of isotopically light Zn sulfides is the main cause of isotopic variation in hydrothermal fluids studied here. A few studies have identified or inferred the preferential incorporation of lighter Zn isotopes into Zn sulfide precipitates (e.g. Wilkinson et al., 2005). Laboratory experiments have also demonstrated sulfide precipitation accompanied by an isotope effect of Δ^{66}Zn = −0.36‰ (Archer et al., 2004). We have determined the isotope effect for Zn sulfide precipitation from vent fluids within Ti-samplers by measuring the δ^{66}Zn of both dissolved and particulate (dregs) Zn in samples recovered from the Ti-sampler from K-vent and Bio9'' (Section 4.1). Because these fluids were observed to be clear when they exited the vent, we presume that the particulates formed in the sampler as the fluids cooled in the sampler. For fluids from K-vent, we calculate isotope effects of Δ^{66}Zn = −0.87‰ for sample W1, and Δ^{66}Zn = −0.76‰ for sample W2 for sulfide precipitation in the samplers. The isotope effect for sulfide precipitation in the Bio9'' samples was Δ^{66}Zn = 0. The reason for this absence of isotopic fractionation is not known, though it may reflect

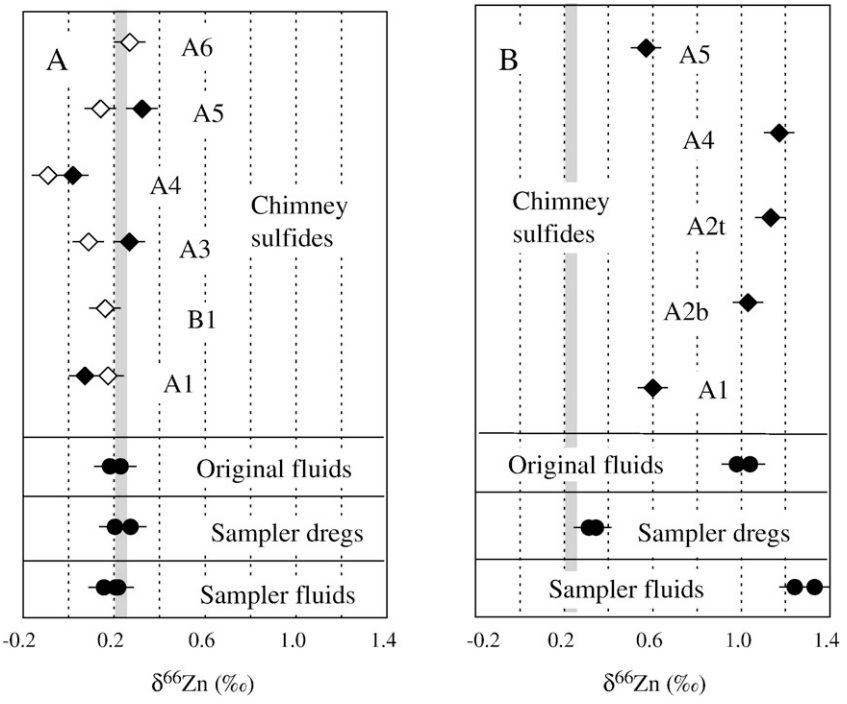

Fig. 4. Fluid and chimney sulfide δ^{66}Zn from (A) Bio9'' (383 °C) and (B) K-vent (203 °C) at 9–10°N on the EPR. At several places in the Bio9'' chimney, the δ^{66}Zn from nearby minerals which were predominantly chalcopyrite (◊) and predominantly sphalerite (♦) were compared. The Zn isotope composition of the original hydrothermal fluids (the fluids venting at the seafloor) was reconstructed as the sum of Zn isotopes in the fluids and dregs recovered from each sampler (Section 4.1).

differences in the mineralogy of the sulfide precipitates, or differences in kinetic and/or equilibrium isotope effects during sulfide precipitation. Isotope effects may be overwhelmed by rapid precipitation of sulfides during the cooling of fluids within the samplers and therefore may not be directly comparable to the fractionation that would occur during subsurface precipitation when fluids are cooled more slowly. Finally, a negative isotope effect for sulfide precipitation can be seen in a comparison of fluids and chimney sulfides from the same location, where (within analytical error) chimney sulfide δ^{66}Zn is similar to or isotopically lighter than fluids from the same vent (Fig. 4). Assuming that the *in situ* isotope effect for subsurface sulfide precipitation is negative, isotopically heavy fluids are an indication that subsurface Zn sulfide precipitation has occurred. The absence of Zn isotope fractionation in hydrothermal fluids compared to source rocks may result either from the absence of isotopic fractionation during subsurface sulfide precipitation (Δ^{66}Zn = 0) or the absence of subsurface Zn sulfide precipitation.

Physical and chemical measurements are consistent with our hypothesis that the primary cause of Zn isotope variations in hydrothermal fluids is subsurface precipitation of isotopically light Zn sulfides. Fluid temperatures, Fe/Mn ratios, and Cu concentrations are low in all of the fluid samples with the highest δ^{66}Zn values (Table 1, Supplementary data). Temperature has a large impact on sphalerite solubility, which decreases by as much as three orders of magnitude between 350 °C and 200 °C in modeled hydrothermal fluids (Tivey et al., 1999). Also, Fe is rapidly precipitated when hydrothermal fluids cool whereas Mn is conservative during fluid cooling, so low Fe/Mn ratios are an indicator of subsurface metal sulfide precipitation (Seewald and Seyfried, 1990). The fact that Cu and, to a lesser extent Zn, concentrations in the end-member fluids display a sharp decrease with temperature below 350 °C is consistent with previous studies (Metz and Trefry, 2000) and may reflect Cu-and Zn-sulfide precipitation in subsurface during cooling of the hydrothermal fluid. Thus, the relationship between fluid temperature and δ^{66}Zn may reflect the large impact that temperature has on Zn sulfide solubility.

While samples from the TAG hydrothermal field do not noticeably deviate from the correlation between fluid temperature and δ^{66}Zn observed at the EPR, the relationship between temperature and sphalerite solubility in these region can be more complicated. Particularly, the white smokers at the TAG site are known to contain a high concentration of "remobilized" Zn (Edmond et al., 1995; Tivey et al., 1995). Subsurface precipitation of Fe sulfides lowers the pH of fluids in white smoker hydrothermal systems. These lower-pH fluids can then redissolve Zn sulfides that were precipitated earlier in the history of the vents. Therefore, we expect that the δ^{66}Zn of white smoker fluids will be significantly affected by the δ^{66}Zn of subsurface Zn sulfides that formed earlier in the history of the vent system. The δ^{66}Zn values for white smoker fluids range from +0.13‰ to +0.41‰, similar to the range for black smoker fluids, suggesting that Zn sulfides precipitated earlier in the history of these vents were not significantly fractionated from vent fluids, either because the instantaneous isotope effect for precipitation was small or because Zn precipitation was near-quantitative.

4.3. Results of thermodynamic modeling

Thermodynamic calculations using vent fluid compositions further supports our hypothesis that subsurface Zn sulfide precipitation is the primary cause of isotopically heavy hydrothermal vent fluids. We have observed a positive correlation between calculated sphalerite saturation and δ^{66}Zn in hydrothermal fluids (Fig. 3). The only fluid that, according to our calculations, is saturated with respect to sphalerite at measured vent exit temperatures is K-vent at 9–10°N EPR. The +1.0‰ δ^{66}Zn values for K-vent fluids are the isotopically heaviest in this study, consistent with subsurface precipitation of isotopically light sphalerite. Isotopically heavy δ^{66}Zn values are also observed in fluids from the NGS site at 21°N on the EPR. δ^{66}Zn values for NGS vary from +0.25‰ to +0.65‰. Although speciation calculations for the measured fluid composition at NGS indicate that this fluid is undersaturated with respect to sphalerite, fluids from NGS are closer to saturation than other samples from 21°N EPR. The heavier δ^{66}Zn values observed here may indicate that Zn sulfides are supersaturated within the subsurface hydrothermal vent system under conditions not represented by the model. Alternatively, the heavy and variable δ^{66}Zn values of NGS fluids may be due to sampling artifacts. Zn isotope data reported here are for replicate fluid samples collected from a single sulfide chimney orifice at NGS. Scatter in the major and trace-element data (Von Damm, 1983) suggests non-conservative behavior of chalcophile (e.g., Fe, Cu, Zn, etc.) elements during sampling. This is likely due to entrainment of ambient seawater into the Ti-sampler as evidenced by variable Mg content of recovered fluids (up to 17 mM). Seawater entrainment (and/or conductive cooling) during sampling commonly results in sulfide (dregs) precipitation within samplers. Zn-sulfide precipitation within samplers at NGS would remove variable amounts of isotopically-light Zn from solution, reducing the concentration of dissolved Zn whilst increasing the residual δ^{66}Zn of the fluid. Precipitate (dregs) fractions for fluids from NGS are not available for this study.

Fluid speciation calculations indicate under-saturation with respect to Zn-sulfide at *in situ* conditions for all other vent areas. The fluids from all these areas have δ^{66}Zn values not significantly heavier than the primary volcanics (+0.19 to +0.30‰), suggesting that hydrothermal fluids have not deposited significant amounts of Cu–Fe-and/or Zn-sulfide.

4.4. Paired mineral and fluid Zinc isotopes

4.4.1. Bio9" high-temperature vent

Chimney minerals from the Bio9'' vent include sphalerite with variable amounts of chalcopyrite and pyrite and have an isotopic composition similar to the vent fluids (Fig. 4A). The average Zn isotope composition of the fluids was δ^{66}Zn = +0.21‰, compared to +0.13‰ for the minerals sampled. The similarity between the δ^{66}Zn of vent fluids and basalt (see Section 4.2) suggests that Zn isotopes are not fractionated as Zn is leached from basalt source rocks and travels up to the ocean floor through the hydrothermal system. These results are consistent with minimal subsurface precipitation of Zn sulfides

at this site as predicted by thermodynamic calculations; Bio9" is undersaturated with respect to Zn sulfide.

Individual mineral samples from the Bio9'' vent range from δ^{66}Zn=−0.09‰ to +0.32‰. These values represent real differences in Zn isotopes, because the range is much larger than our analytical uncertainty. Yet, there is no clear relationship between δ^{66}Zn and location, mineralogy and/or paragenesis of sphalerite in the chimney that would allow us to determine what process is responsible for the observed differences. Changes in δ^{66}Zn of the fluid precipitating Zn-sulfide in different locations across the chimney wall might be responsible. However, quantitative models of fluid transport and chemical reaction demonstrate transport-dominated environments within black smoker chimney walls (Tivey, 1995a) and thus reservoir (Rayleigh fractionation) effects are not likely to dominate. Variability of Zn isotopic fractionation (kinetic *versus* equilibrium) during sulfide precipitation or temporal variations in fluid δ^{66}Zn may be more likely.

Our data do not show the same relationship between Zn isotopes in co-existing sphalerite and chalcopyrite samples as observed in previous studies: chalcopyrite δ^{66}Zn samples were around 0.4‰ lighter than nearby sphalerite in samples from the Alexandrinka deposit in Russia (Mason et al., 2005). Although we find that chalcopyrite is lighter in two of the four locations sampled, the maximum difference between $\delta^{66}Zn_{sphalerite}$ and $\delta^{66}Zn_{chalcopyrite}$ is only 0.18‰. At two locations in the chimney the sphalerite and the chalcopyrite were equal within analytical error. This disparity may result from the fact that Zn-enrichment in chalcopyrite at Bio9" results mainly from fine-grained inclusion of sphalerite within the chalcopyrite matrix while Zn-enrichment in chalcopyrite studied by Mason et al. (2005) is believed to result from lattice substitution. Differences in the local conditions under which the minerals precipitated may also explain such differences. While the minerals studied by Mason et al. (2005) were formed deep within the hydrothermal stock work, our samples were taken from a chimney where minerals most likely precipitated much more quickly as vent fluids mixed with seawater. The equilibrium isotope effect for Zn-sulfide precipitation may be different for the hydrothermal conditions by which our samples were formed, or rapid precipitation may have made isotopic equilibration impossible.

4.4.2. K-vent low-temperature vent

The Zn-isotopic composition of chimney minerals at this vent site range from δ^{66}Zn=+0.57‰ to +1.17‰; a greater range than at the high-temperature vent Bio 9" and much heavier than the likely δ^{66}Zn in basalt source rocks (Fig. 4B). δ^{66}Zn of the reconstructed venting fluids, calculated as the sum of Zn isotopes in fluids and particulates recovered from the samplers, were +1.04‰ and +0.98‰ for the duplicate samples (Section 4.1). We believe that minerals at this site are isotopically heavy largely because they precipitate from isotopically heavy fluids.

The variability of δ^{66}Zn values observed among sulfide minerals in the K-vent chimney may result from temporal variations in the fluid δ^{66}Zn, or variations in the precipitation isotope effect. Temporal variations in the amount of subsurface Zn sulfide precipitation at this site could have lead to temporal variations in the fluid δ^{66}Zn. This may explain why some sulfides appear to be slightly heavier than hydrothermal fluids sampled at this vent (although they are in fact indistinguishable within analytical error). Alternatively, differences in the precipitation isotope effect could lead to variations in sulfide δ^{66}Zn even if fluid δ^{66}Zn was constant during the life of the chimney. While K-vent samples are composed of sphalerite with variable enrichment of marcasite, pyrite and galena, Zn is hosted primarily in sphalerite and it is unlikely that changes of δ^{66}Zn values result from changes in sulfide mineralogy. Instead, it is possible that different samples of sphalerite in the K-vent structure precipitated under different conditions. Sub-samples A1 and A2 were recovered from the base of the chimney within a well-developed conduit wall. In contrast, sub-samples A4 and A5 were recovered from the porous beehive structure forming the upper part of the chimney. Although, there is no systematic relation between location of the sample (i.e., interior *versus* exterior sections of chimney wall; see Rouxel et al., in press) and the corresponding δ^{66}Zn, variations of δ^{66}Zn values of chimney sulfide may result from local effects during sphalerite precipitation. Although equilibrium Zn-isotope fractionation in sphalerite has not been determined experimentally or calculated theoretically, minimal or slightly positive Zn-isotope fractionation factors (up to 0.1‰) between sphalerite and vent fluid could result from near-equilibrium isotope effects during Zn-sulfide precipitation. In contrast, negative Zn-isotope fractionation factors (down to −0.4‰) are consistent with kinetic Zn-isotope effects during sphalerite precipitation as previously observed by Archer et al. (2004). The fact that rapidly precipitated sulfides formed during fluid sampling at K-vent (dregs) have lower δ^{66}Zn values by about 0.9‰ compared to vent fluid is also consistent with this model.

4.5. The hydrothermal Zn isotope budget

Zn in hydrothermal vent fluids may impact on the δ^{66}Zn of seawater. The mid-ocean ridge hydrothermal Zn flux has been estimated to be 1300% of the natural riverine flux (Wheat et al., 2002). Estimates of ocean cycling time through hydrothermal plumes are several thousand years (Elderfield and Schultz, 1996), on the order of the residence time of the deep ocean. Much of the Zn in hydrothermal vent fluids precipitates quickly as metal sulfides in the region near the vent, but some may remain in hydrothermal plumes either as particles or dissolved Zn (German et al., 1991). Significant amounts of isotopic exchange between hydrothermal-origin Zn and deep-water Zn in hydrothermal plumes could therefore affect the δ^{66}Zn of seawater. We estimate the riverine and atmospheric input of Zn to the ocean to have a δ^{66}Zn isotopic composition between +0.1‰ and +0.3‰. This range encompasses measurements of Zn isotopes in basalts, Niger dust (Maréchal et al., 2000), an average of four reference ores (Chapman et al., 2006), and measurements of most common anthropogenic Zn products (John et al., 2007). When hydrothermal fluids mix with seawater, additional isotopically-light Zn may be lost into sulfide precipitates, so Zn in hydrothermal plumes could be even heavier than hydrothermal fluids exiting at the seafloor. We have measured the isotopic composition of deep Pacific seawater to be δ^{66}Zn=+0.46‰ (John et al., 2005),

heavier than our estimated riverine and atmospheric input. Hydrothermal processes could be responsible for this difference.

5. Conclusions

We have presented the first data on Zn isotopes in modern hydrothermal systems and the first data on Zn isotopes in hydrothermal vent fluids. Our data suggest that the subsurface precipitation of Zn sulfides is the most important factor in altering the δ^{66}Zn of hydrothermal vent fluids. In hydrothermal systems where there is little subsurface sulfide precipitation, the δ^{66}Zn of hydrothermal fluids matches the expected δ^{66}Zn of basalt source rocks. In hydrothermal systems where significant amounts of subsurface sulfide precipitation is predicted, preferential incorporation of lighter Zn isotopes into Zn-bearing sulfide mineral appears to be associated with the development of isotopically heavy hydrothermal fluids.

With a better understanding of how Zn isotopes are fractionated in hydrothermal systems, Zn isotopic analysis may be a tool to help us understand the plumbing and chemistry of hydrothermal systems. Subsurface hydrothermal conditions can be difficult to predict based on analysis of seafloor hydrothermal fluids, as subsurface precipitation and redissolution of minerals changes fluid chemistry. As we are able to better constrain the isotope effect for Zn sulfide precipitation under hydrothermal conditions, Zn isotopes may be used to calculate the extent of Zn sulfide precipitation or remobilization in different fluids. Such a proxy for sulfide precipitation could provide valuable insight into hydrothermal processes.

Acknowledgements

John Edmond, Karen Von Damm, Katrina Edwards, Wolfgang Bach, the captain and crews of R/V Atlantis and Alvin, and all others who contributed to collection of these samples are thanked for their efforts. Karen Von Damm and Andy Campbell provided supplementary data on many of the hydrothermal fluid samples. Meg Tivey provided guidance on the thermodynamic calculations presented here and several helpful conversations on interpreting our data. Francis Albarede, Derek Vance, and an anonymous reviewer provided valuable comments that improved the manuscript.

This work was supported by NSF grants OCE-0326689, OCE-0327448, OCE-0241791, the MIT Martin Family Society of Fellows for Sustainability, and the WHOI Ocean Ventures Fund and Deep Ocean Exploration Institute.

Appendix A. Supplementary data

Supplementary data associated with this article can be found, in the online version, at doi:10.1016/j.epsl.2007.12.011.

References

Albarède, F., 2004. The stable isotope geochemistry of copper and zinc. Geochemistry of Non-Traditional Stable Isotopes, pp. 409–427.

Albarède, F., Beard, B., 2004. Analytical Methods for Non-Traditional Isotopes, Geochemistry of Non-Traditional Stable Isotopes, pp. 113–152.

Anbar, A.D., Rouxel, O.J., 2007. Metal isotopes in paleoceanography. Annu. Rev. Earth Planet. Sci 35, 717–746.

Archer, C., Vance, D., 2002. Large fractionations in Fe, Cu and Zn isotopes associated with Archean microbially-mediated sulphides. Geochim. Cosmochim. Acta 66 (15A), A26.

Archer, C., Vance, D., 2004. Mass discrimination correction in multiple-collector plasma source mass spectrometry: an example using Cu and Zn isotopes. J. Anal. At. Spectrom. 19, 656–665.

Archer, C., Vance, D., Butler, I., 2004. Abiotic Zn isotope fractionations associated with ZnS precipitation. Geochim. Cosmochim. Acta 68 (11), A325.

Ben Othman, D., Luck, J.M., Tchalikian, A., Albarède, F., 2003. Cu-Zn isotope systematics in terrestrial basalts. Geophys. Res. Abstr. 5, 09669.

Bermin, J., Vance, D., Archer, C., Statham, P.J., 2006. The determination of the isotopic composition of Cu and Zn in seawater. Chem. Geol. 226 (3–4), 280–297.

Campbell, A.C., Bowers, T.S., Measures, C.I., Falkner, K.K., Khadem, M., Edmond, J.M., 1988. A time-series of vent fluid compositions from 21-degrees-N, East Pacific Rise (1979, 1981, 1985), and the Guaymas Basin, Gulf of California (1982, 1985). J. Geophys. Res.-Solid Earth Planets 93 (B5), 4537–4549.

Chapman, J.B., Mason, T.F.D., Weiss, D.J., Coles, B.J., Wilkinson, J.J., 2006. Chemical separation and isotopic variations of Cu and Zn from five geological reference materials. Geostand. Geoanal. Res. 30 (1), 5–16.

Ding, K., Seyfried, W.E., 1992a. Determination of Fe–Cl complexing in the low-pressure supercritical region (Nacl fluid) — iron solubility constraints on ph of subseafloor hydrothermal fluids. Geochim. Cosmochim. Acta 56 (10), 3681–3692.

Ding, K., Seyfried, W.E., 1992b. Experimental determination of Cu–Cl speciation at the T-P conditions relevant to ridge crest hydrothermal activity: implications to log(fO2) in the hot spring fluids. Eos Trans., AGU 73 (43) Fall Meeting Suppl. 254.

Edmond, J.M., Campbell, A.C., Palmer, M.R., Klinkhammer, G.P., German, C.R., Edmonds, H.N., Elderfield, H., Thompson, G., Rona, P.A., 1995. Time series studies of vent fluids from the TAG and MARK sites (1986, 1990) mid-Atlantic ridge: a new solution chemistry model and a mechanism of Cu/Zn zonation in massive sulphide orebodies. In: Parson, C.L.W.L.M., Dixon, D.R. (Eds.), Hydrothermal Vents and Processes. Geol. Soc. Special Publ., pp. 77–86.

Elderfield, H., Schultz, A., 1996. Mid-ocean ridge hydrothermal fluxes and the chemical composition of the ocean. Annu. Rev. Earth Planet. Sci. 24, 191–224.

Fornari, D.J., Shank, T., VonDamm, K.L., Gregg, T.K.P., Lilley, M., Levai, G., Bray, A., Haymon, R.M., Perfit, M.R., Lutz, R., 1998. Time-series temperature measurements at high-temperature hydrothermal vents, East Pacific Rise 9°49'–51'N: evidence for monitoring a crustal cracking event. Earth Planet. Sci. Lett. 160, 419–431.

Galer, S.J.G., 1999. Optimal double and triple spiking for high precision lead isotopic measurement. Chem. Geol. 157 (3–4), 255–274.

German, C.R., Campbell, A.C., Edmond, J.M., 1991. Hydrothermal scavenging at the mid-Atlantic ridge — modification of trace-element dissolved fluxes. Earth Planet. Sci. Lett. 107 (1), 101–114.

Haymon, R.M., Fornari, D.J., Damm, K.L.V., Lilley, M.D., Perfit, M.R., Edmond, J.M., Shanks, W.C., Lutz, R.A., Grebmeier, J.M., Carbotte, S., Wright, D., McLaughlin, E., Smith, M., Beedle, N., Olson, E., 1993. Volcanic eruption of the mid-ocean ridge along the East Pacific Rise crest at 9°45–52? N: direct submersible observations of seafloor phenomena associated with an eruption event in April, 1991. Earth Planet. Sci. Lett. 119, 85–101.

Haymon, R.M., Fornari, D.J., Edwards, M.H., Carbotte, S., Wright, D., Macdonald, K.C., 1991. Hydrothermal vent distribution along the East Pacific Rise crest (9'09–54N) and its relationship to magmatic and tectonic processes on fast-spreading mid-ocean ridges. Earth Planet. Sci. Lett 104, 513–534.

John, S.G., Bergquist, B.A., Saito, M.A., Boyle, E.A., 2005. Zinc isotope variations in phytoplankton and seawater. Geochim. Cosmochim. Acta 69 (10), A546.

John, S.G., Park, G., Zhang, Z., Boyle, E.A., 2007. The isotopic composition of some common forms of anthropogenic zinc. Chem. Geol. 245 (1–2), 61–69.

Johnson, C., Beard, B., Albarède, F. (Eds.), 2004. Geochemistry of non-traditional stable isotopes. Rev. Mineral. Geochem., vol. 55.

Johnson, J.W., Oelkers, E.H., Helgeson, H.C., 1992. Supcrt92 — a software package for calculating the standard molal thermodynamic properties of

minerals, gases, aqueous species, and reactions from 1-Bar to 5000-Bar and 0-Degrees-C to 1000-Degrees-C. Comput. Geosci. 18 (7), 899–947.

Kraus, K.A., Moore, G.E., 1953. Anion exchange studies. VI. The dIvalent transition elements manganese to zinc in hydrochloric acid. J. Am. Chem. Soc. 75, 1457–1460.

Maréchal, C.N., Nicolas, E., Douchet, C., Albarède, F., 2000. Abundance of zinc isotopes as a marine biogeochemical tracer. Geochem. Geophys. Geosystems vol. 1, GC000029 1999.

Maréchal, C.N., Telouk, P., Albarède, F., 1999. Precise analysis of copper and zinc isotopic compositions by plasma-source mass spectrometry. Chem. Geol. 156 (1–4), 251–273.

Mason, T.F.D., Weiss, D.J., Chapman, J.B., Wilkinson, J.J., Tessalina, S.G., Spiro, B., Horstwood, M.S.A., Spratt, J., Coles, B.J., 2005. Zn and Cu isotopic variability in the Alexandrinka volcanic-hosted massive sulphide (VHMS) ore deposit, Urals, Russia. Chem. Geol. 221 (3–4), 170–187.

McCollom, T.M., Shock, E.L., 1997. Geochemical constraints on chemo-lithoautotrophic metabolism by microorganisms in seafloor hydrothermal systems. Geochim. Cosmochim. Acta 61 (20), 4375–4391.

McManus, J., Nagler, T.F., Siebert, C., Wheat, C.G., Hammond, D.E., 2002. Oceanic molybdenum isotope fractionation: diagenesis and hydrothermal ridge-flank alteration. Geochem. Geophys. Geosystems vol 3 Art. No. 1078.

Metz, S., Trefry, J.H., 2000. Chemical and mineralogical influences on concentrations of trace metals in hydrothermal fluids. Geochim. Cosmochim. Acta 64, 2267–2279.

Peng, X., Zhou, H., 2005. Growth history of hydrothermal chimneys at EPR 9–10°N: A structural and mineralogical study. Sci. China, Ser. D Earth Sci. 48, 1891–1899.

Pichat, S., Douchet, C., Albarède, F., 2003. Zinc isotope variations in deep-sea carbonates from the eastern equatorial Pacific over the last 175 ka. Earth Planet. Sci. Lett. 210 (1–2), 167–178.

Rouxel, O., Fouquet, Y., Ludden, J.N., 2004a. Copper isotope systematics of the Lucky Strike, Rainbow, and Logatchev sea-floor hydrothermal fields on the Mid-Atlantic Ridge. Econ. Geol. 99 (3), 585–600.

Rouxel, O., Fouquet, Y., Ludden, J.N., 2004b. Subsurface processes at the Lucky Strike hydrothermal field, Mid-Atlantic Ridge: evidence from sulfur, selenium, and iron isotopes. Geochim. Cosmochim. Acta 68 (10), 2295–2311.

Rouxel, O., Ludden, J., Fouquet, Y., 2003. Antimony isotope variations in natural systems and implications for their use as geochemical tracers. Chem. Geol. 200 (1–2), 25–40.

Rouxel, O., Shanks, W.C., Bach, W., Edwards, K.J., in press. Integrated Fe and S isotope study of seafloor hydrothermal vents at East Pacific Rise 9–10°N. Submitted to Chemical Geology.

Seewald, J.S., Seyfried, W.E., 1990. The effect of temperature on metal mobility in subseafloor hydrothermal systems — constraints from basalt alteration experiments. Earth Planet. Sci. Lett. 101 (2–4), 388–403.

Seewald, J.S., Seyfried, W.E., Shanks, W.C., 1994. Variations in the chemical and stable isotope composition of carbon and sulfur species during organic-rich sediment alteration: an experimental and theoretical study of hydrothermal activity at Guaymas basin, gulf of California. Geochim. Cosmochim. Acta 58 (22), 5065–5082.

Severmann, S., Johnson, C.M., Beard, B.L., German, C.R., Edmonds, H.N., Chiba, H., Green, D.R.H., 2004. The effect of plume processes on the Fe isotope composition of hydrothermally derived Fe in the deep ocean as inferred from the Rainbow vent site, Mid-Atlantic Ridge, 36 degrees 14' N. Earth Planet. Sci. Lett. 225 (1–2), 63–76.

Shank, T.M., Fornari, D.J., Damm, K.L.V., Lilley, M.D., Haymon, R.M., Lutz, R.A., 1998. Temporal and spatial patterns of biological community development at nascent deep-sea hydrothermal vents (9'50N, East Pacific Rise). Deep-Sea Res. II 45, 465–515.

Sharma, M., Polizzotto, M., Anbar, A.D., 2001. Iron isotopes in hot springs along the Juan de Fuca Ridge. Earth Planet. Sci. Lett. 194 (1–2), 39–51.

Sverjensky, D.A., Hemley, J.J., Dangelo, W.M., 1991. Thermodynamic assessment of hydrothermal alkali feldspar-mica-aluminosilicate equilibria. Geochim. Cosmochim. Acta 55 (4), 989–1004.

Tivey, M.K., 1995a. The influence of hydrothermal fluid composition and advection rates on black smoker chimney mineralogy — insights from modeling transport and reaction. Geochim. Cosmochim. Acta 59 (10), 1933–1949.

Tivey, M.K., 1995b. The influence of hydrothermal fluid composition and advection rates on black smoker chimney mineralogy: insights from modeling transport and reaction. Geochim. Cosmochim. Acta 59, 1933–1949.

Tivey, M.K., Humphris, S.E., Thompson, G., Hannington, M.D., Rona, P.A., 1995. Deducing patterns of fluid-flow and mixing within the TAG active hydrothermal mound using mineralogical and geochemical data. J. Geophys. Res.-Solid Earth 100 (B7), 12527–12555.

Tivey, M.K., Stakes, D.S., Cook, T.L., Hannington, M.D., Petersen, S., 1999. A model for growth of steep-sided vent structures on the Endeavour Segment of the Juan de Fuca Ridge: results of a petrologic and geochemical study. J. Geophys. Res.-Solid Earth 104 (B10), 22859–22883.

Von Damm, K.L., 1983. Chemistry of Submarine Hydrothermal Solutions at 21° North, East Pacific Rise and Guaymas Basin, Gulf of California. Massachusetts Institute of Technology, Cambridge, Massachusetts. 240 pp.

Von Damm, K.L., 2000. Chemistry of hydrothermal vent fluids from 9 degrees–10 degrees N, East Pacific Rise: "Time zero", the immediate posteruptive period. J. Geophys. Res.-Solid Earth 105 (B5), 11203–11222.

Von Damm, K.L., 2004. Evolution of the hydrothermal system at East Pacific Rise 9°50'N: geochemical evidence for changes in the Upper Oceanic Crust. Mid-Ocean Ridges: Hydrothermal Interactions Between the Lithosphere and Ocean. AGU Monograph, vol. 148.

Von Damm, K.L., Buttermore, L.G., Oosting, S.E., Bray, A.M., Fornari, D.J., Lilley, M.D., Shanks, W.C., 1997. Direct observation of the evolution of a seafloor 'black smoker' from vapor to brine. Earth Planet. Sci. Lett. 149 (1–4), 101–111.

Von Damm, K.L., Edmond, J.M., Grant, B., Measures, C.I., 1985a. Chemistry of submarine hydrothermal solutions at 21-degrees-N, east pacific rise. Geochim. Cosmochim. Acta 49 (11), 2197–2220.

Von Damm, K.L., Edmond, J.M., Measures, C.I., Grant, B., 1985b. Chemistry of submarine hydrothermal solutions at Guaymas Basin, Gulf of California. Geochim. Cosmochim. Acta 49 (11), 2221–2237.

Von Damm, K.L., Lilley, M.D., 2004. Diffuse flow hydrothermal fluids from 9°50' N East Pacific Rise: origin, evolution and biogeochemical controls. In: Wilcock, W.S.D., DeLong, E.F., Kelley, D.S., Baross, J.A., Cary, S.C. (Eds.), The Subseafloor Biosphere at Mid-Ocean Ridges. AGU Monograph, pp. 245–268.

Weiss, D.J., Mason, T.F.D., Zhao, F.J., Kirk, G.J.D., Coles, B.J., Horstwood, M.S.A., 2005. Isotopic discrimination of zinc in higher plants. New Phytol. 165 (3), 703–710.

Welhan, J.A., Craig, H., 1983. Methane, hydrogen and helium in hydrothermal fluids at 21°N on the East Pacific Rise. In: Rona, P., Bostrom, K., Laubier, L., Smith, K.L. (Eds.), Hydrothermal Processes at Seafloor Spreading Centers. Plenum Press, London, pp. 391–409.

Wheat, C.G., Mottl, M.J., Rudnicki, M., 2002. Trace element and REE composition of a low-temperature ridge-flank hydrothermal spring. Geochim. Cosmochim. Acta 66 (21), 3693–3705.

Wilkinson, J.J., Weiss, D.J., Mason, T.F.D., Coles, B.J., 2005. Zinc isotope variation in hydrothermal systems: preliminary evidence from the Irish Midlands ore field. Econ. Geol. 100 (3), 583–590.

Wolery, T.J., 1992. EQ3NR, A Computer Program for Geochemical Aqueous Speciation-Solubility Calculations: Theoretical Manual, User's Guide, and Related Documentation (Version 7.0). Lawrence Livermore Natl. Lab, Livermore, CA.

Wolery, T.J., Daveler, S.A., 1992. EQ6, A Computer Program for Reaction Path Modeling of Aqueous Geochemical Systems: Theoretical Manual, User's Guide, and Related Documentation (Version 7.0). Livermore, CA, Lawrence Livermore Natl. Lab.

Zhu, X.K., O'Nions, R.K., Guo, Y., Belshaw, N.S., Rickard, D., 2000. Determination of natural Cu-isotope variation by plasma-source mass spectrometry: implications for use as geochemical tracers. Chem. Geol. 163 (1–4), 139–149.